

# THE STRUCTURE OF NEUTRON-RICH NUCLEI STUDIED BY DEEP INELASTIC REACTIONS: RECENT RESULTS FROM LNL\*

GIACOMO DE ANGELIS

INFN Laboratori Nazionali di Legnaro  
viale dell'Università 2, 35020 Legnaro, Italy

*(Received February 21, 2011)*

The evolution of nuclear properties as a function of the neutron excess depends on how the shell structure changes. This evolution has consequences on the ground state properties and on the single-particle and collective excitations. Presently, our knowledge about the structure of nuclei is mostly limited to nuclei close to the valley of stability or nuclei with a deficiency of neutrons. Only recently the availability of beams of unstable ions has given access to unexplored regions of the nuclear chart, especially on the neutron-rich side. A complementary way to study the structure of neutron-rich nuclear systems is offered by the use of high intensity beams of stable ions and binary reactions. Multi-nucleon and deep-inelastic reactions are a powerful tool to populate medium- and high-spin states in moderately neutron-rich systems. In this article, I will discuss some selected examples studied using the novel experimental setup that combines the large acceptance magnetic spectrometer, PRISMA, and the high-efficiency  $\gamma$ -ray detection arrays, CLARA and AGATA. They show the high potential of such reaction mechanism for the study of the spectroscopic properties of neutron-rich nuclear systems.

DOI:10.5506/APhysPolB.42.519

PACS numbers: 23.20.Lv, 25.70.Lm, 27.40.+z

## 1. Introduction

The magic numbers in the atomic nucleus represent a fundamental quantity governing nuclear structure. Magic numbers originate from the large shell gaps in the energy spectrum of single-particle states. They can be reproduced using a single-particle harmonic oscillator potential with a strong spin-orbit interaction. However, since single particle energies change with

---

\* Presented at the Zakopane Conference on Nuclear Physics “Extremes of the Nuclear Landscape”, August 30–September 5, 2010, Zakopane, Poland.

increasing neutron excess, it becomes essential to probe their evolution in the neutron-rich regions of the nuclear chart. Binary reactions such as multi-nucleon transfer and deep-inelastic collisions have proven since long to be a useful tool to populate neutron-rich nuclei at relatively high angular momentum [1]. Most recently, the use of efficient gamma-ray detector arrays coupled to large-acceptance magnetic spectrometers has allowed to easily associate the observed  $\gamma$ -rays to a specific nucleus [2]. Due to the peculiar reaction mechanism, spectroscopic information obtained in this way is often complementary to that provided by first generation radioactive beam facilities. There is by now a vast evidence that substantial changes in the shell structure of atomic nuclei occur when adding neutrons: the relative energies of single particle orbitals evolve as a function of neutron number leading to modifications of the well established magic numbers. As a consequence, new regions of deformation develop for nucleon numbers that, close to the stability, are considered “magic”. Such evolution of the shell structure has been recently related to the effect of the tensor part of the nucleon–nucleon interaction [3]. The tensor-force, one of the most direct manifestation of the meson exchange origin of the nucleon–nucleon interaction, is responsible for the strong attraction between a proton and a neutron in the spin-flip partner orbits. A recent generalization of such mechanism foresees a similar behavior also for orbitals with non-identical orbital angular momenta. An attraction is expected for orbitals with antiparallel spin configuration, whereas orbitals with parallel spin configuration should repel each other [4]. In the neutron-rich nuclei with  $A \approx 40$ –80 all these physics issues can be addressed: the excited structures of nuclei in the  $N = 20$ –28 region have been used to test the prediction of new effective interactions. A new sub-shell closure at  $N = 32$  has been identified [5], whereas the known sub-shell closure at  $N = 40$ , evident at  $Z = 28$ , disappears by removing two or four protons from the spherical  $^{68}\text{Ni}$  what drives the  $N = 40$  nuclei  $^{66}\text{Fe}$  and  $^{64}\text{Cr}$  into deformed shapes. Furthermore, there are predictions of a new sub-shell closure at  $N = 34$  for Ca nuclei and the quenching of the  $N = 50$  gap towards  $^{78}\text{Ni}$ . In this paper, I will briefly review some of the results on neutron-rich nuclei in the mass range 40–80 obtained from experiments performed at the Legnaro National Laboratories (LNL) by bombarding a  $^{238}\text{U}$  target with the most neutron-rich beams available in nature. Data have been taken using the CLARA and AGATA  $\gamma$ -ray detector arrays [6] in coincidence with the PRISMA spectrometer [7] as well as with others ancillary detectors. The experimental data are discussed and interpreted in the framework of large shell-model calculations using newly developed effective interactions.

### 1.1. The $N = 20$ – $28$ isotones and the “island of inversion”

The region of neutron-rich nuclei around  $N = 20$ – $28$ , where the breaking of a shell closure far from stability was first observed in  $^{32}\text{Mg}$ , continues to be a subject of active research both experimental and theoretical. Within a shell model context such breaking was interpreted as arising from a two particle–two hole intruder configuration [8]. The neutron-rich S, P and Si nuclei have been populated using the  $^{36}\text{S}$  on  $^{208}\text{Pb}$  reaction. The excited structures of  $^{40}\text{S}$  [9],  $^{33}\text{Si}$  [10] and  $^{38}\text{Cl}$  [11] have been investigated at medium and high spin and compared with the results of large scale  $1\hbar\omega$   $p$ – $sd$ – $pf$  shell model calculations. The results have been used in order to validate the predictions of different residual interaction including in particular the recently developed PSDPFB effective interaction.

### 1.2. The $N = 32$ sub-shell closure from the spectroscopic study of the vanadium isotopes

The neutron-rich vanadium nuclei are among those populated in the  $^{64}\text{Ni} + ^{238}\text{U}$  reaction. From our data, level schemes have been obtained for the  $^{53,55,57}\text{V}$  nuclei and are reported in Ref. [12]. Only in the case of the  $N = 30$  nucleus  $^{53}\text{V}$  excited states were known before this study [13]. The results show that the peak in the  $2^+$  energy observed at  $N = 32$  in the series of Ti isotopes, taken as an indication of a sub-shell closure for this neutron number [14, 15], finds a close correspondence with the peak, again at  $N = 32$ , of the  $11/2^- \rightarrow 7/2^-$  transition energy in the vanadium isotopes. The observed trend of the  $11/2^-$  excitation energy from  $N = 26$  to  $N = 34$  [12] is well reproduced by shell model calculations performed with the code ANTOINE using both the KB3G and GXPF1A effective interactions. From the present results one concludes that the  $N = 32$  sub-shell closure is confirmed in the odd- $Z$   $^{55}\text{V}$  nucleus, but there is no evidence of a  $N = 34$  sub-shell closure in  $^{57}\text{V}$ .

### 1.3. The $N = 34$ sub-shell closure from the study of the $N = 31$ Ca and Sc isotopes

The development of an energy gap at  $N = 34$  in Ca isotopes has also been suggested some time ago [3]. Such gap would arise from a sizeable spacing between the neutron  $p_{1/2}$  and  $f_{5/2}$  at  $Z = 20$  and should be reflected by a relatively high energy of the first excited state,  $2^+$ , in  $^{54}\text{Ca}$ . The gap, however, should disappear at larger  $Z$  values due to a strong  $\pi f_{7/2-\nu} f_{5/2}$  monopole interaction.

On the other end, shell-model calculations with the GXPF1A interaction clearly indicate that a sub-shell closure at  $N = 34$  could appear already in Ti and V isotopes [16], but such predictions have not been confirmed by

the experimental data on the  $N = 34$  nuclei  $^{56}\text{Ti}$  and  $^{57}\text{V}$ . Since it is the above mentioned strong  $\pi f_{7/2}-\nu f_{5/2}$  monopole interaction that, by adding protons in the  $f_{7/2}$  orbital, quenches the  $N = 34$  gap, the effect of adding two or three protons to calcium has apparently been underestimated by the GXPF1A interaction. However, in Ca nuclei the splitting between the  $\nu p_{3/2}$ ,  $\nu p_{1/2}$  and the  $\nu f_{5/2}$  orbitals may still be significant leading to the  $N = 34$  subshell closure. The magnitude of the energy separation between the  $f_{5/2}$  and  $p_{1/2}$  orbitals in neutron-rich Ca isotopes can be derived from studies of the odd  $^{51}\text{Ca}$  by identifying the states involving the  $f_{5/2}$  neutron. The  $^{51}\text{Ca}$  nucleus (as well as the  $^{52}\text{Sc}$  isotone) has been populated by the  $^{48}\text{Ca}$  induced reaction. The observed behavior of the states with predominant  $p_{1/2}$  and  $f_{5/2}$  configurations suggests that the  $p_{1/2}-f_{5/2}$  energy difference in Ca nuclei is above 3 MeV, somewhat smaller than that predicted by the GXPF1A interaction, but still giving rise to a sub-shell closure at  $N = 34$  with a predicted  $2^+$  energy in  $^{54}\text{Ca}$  at around 2.5 MeV [17].

*1.4. Effective charges in the fp shell from lifetime measurements of the neutron-rich  $N = 30$  isotones  $^{50}\text{Ca}$  and  $^{51}\text{Sc}$*

Spectroscopic information on neutron-rich nuclei produced in multi-nucleon transfer reactions has provided so far  $\gamma$ -rays energies,  $\gamma$ - $\gamma$  coincidences and, in some cases, also  $\gamma$ -rays angular distributions or correlations leading to the construction of level schemes for the nuclei of interest. Studies of isomeric states in the nuclei produced in multi-nucleon transfer reactions by employing the thick target technique were limited to isomeric states with lifetimes larger than a few nanoseconds. With the new approach based on a thin target method used in the CLARA-PRISMA setup, it became possible to apply the RDDS technique to measure lifetimes in the  $ps$  range, if the stopper is substituted by a proper energy degrader for the ions entering the PRISMA spectrometer. We have applied for the first time this method to measure lifetimes of excited states in neutron-rich nuclei populated in multi-nucleon transfer reactions. Fig. 1 shows an example of  $\gamma$ -ray spectra taken for different target-degrader distances where, for a single  $\gamma$  transition, two peaks appear corresponding to the decays after and before the degrader, respectively. More details are given in [18, 19]. We were able to extract lifetimes for the first excited states in the  $N = 30$  isotones of Ca and Sc [19] and for the  $^{44,46}\text{Ar}$  nuclei as well [20]. From the data on the  $N = 30$  isotones, effective charges in the  $fp$  shell above  $^{48}\text{Ca}$  have been derived which disagree with those deduced few years ago from the study of proton-rich mirror nuclei [21]. Such result seems to indicate an orbital dependence of the effective charges.

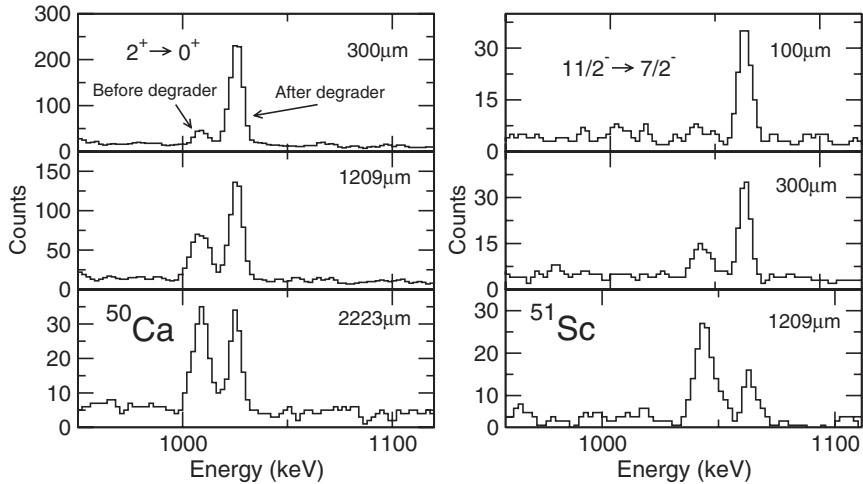


Fig. 1. Doppler-corrected  $\gamma$ -ray spectra showing the  $2^+ \rightarrow 0^+$  1027 keV and the  $11/2^- \rightarrow 7/2^-$  1065 keV transitions in  $^{50}\text{Ca}$  and  $^{51}\text{Sc}$  for different target-degrader distances taken from Ref. [26]. The higher and lower energy peaks correspond to the decay after and before the degrader foil.

### 1.5. Nuclear structure at the $N = 50$ and $Z = 28$ shell closures

Experimental information has been obtained on a wide range of nuclei close to the  $N = 50$  shell closure in the region of  $^{78}\text{Ni}$  using an  $^{82}\text{Se}$  induced reaction. The  $^{238}\text{U}$  target, isotopically enriched, was of a thickness of  $400 \mu\text{g cm}^{-2}$ . Projectile-like nuclei, produced following multi-nucleon transfer and deep inelastic reactions, were detected by the PRISMA spectrometer, placed at an angle of 64 degrees and covering an angular region around the grazing angle of the reaction. Due to the limited  $\gamma$ -coincidence information, for the construction of the level schemes as well as for the spin and parity assignment we have used data obtained in a second experiment performed with the same reaction at the GASP multi-detector array.

Triple and higher-fold  $\gamma$ -coincidences have been acquired in a “thick target” measurement. Here the target, isotopically enriched, was of a thickness of  $60 \text{ mg cm}^{-2}$ , sufficient to stop all reaction fragments. Since all recoiling ions were stopped in the target, Doppler broadening prevented the observation of transitions de-exciting short lived states and only  $\gamma$ -rays originating from states with lifetime longer than the slowing-down time of the recoiling nuclei (1 ps) could be resolved. The spin and parities of the levels were deduced, where possible, from angular distribution ratios of  $\gamma$ -rays from oriented states (ADO) as well as from the decay branchings. Details of the measurements as well as of the data reduction are reported in Ref. [22].

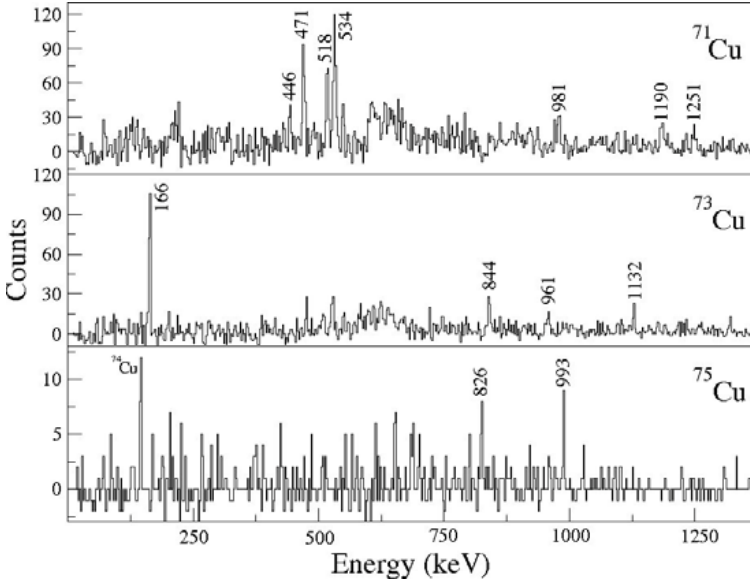


Fig. 2. Mass gated  $\gamma$ -ray spectra of  $^{71}\text{Cu}$ ,  $^{73}\text{Cu}$  and  $^{75}\text{Cu}$  from the data of the  $^{82}\text{Se} + ^{238}\text{U}$  reaction [22].

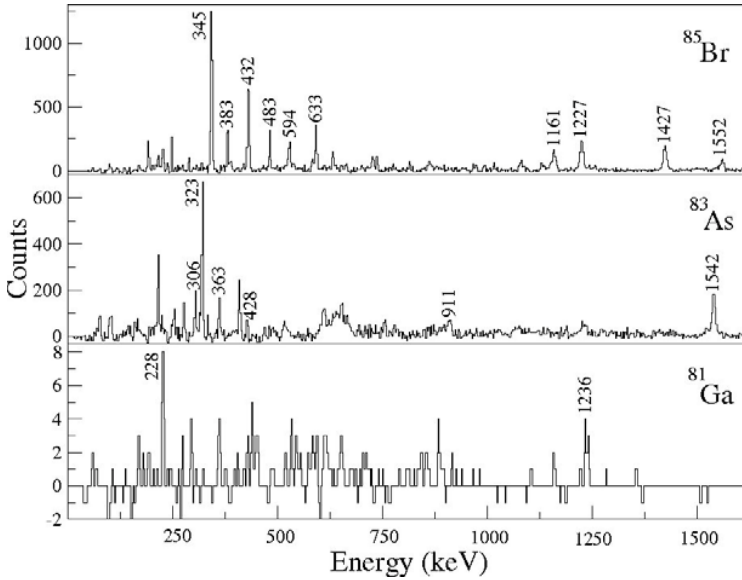


Fig. 3. mass gated  $\gamma$ -ray spectra of  $^{83}\text{As}$ ,  $^{82}\text{Ge}$  and  $^{81}\text{Ga}$  from the data of the  $^{82}\text{Se} + ^{238}\text{U}$  reaction [22].

As an example, Fig. 2 shows the mass gated  $\gamma$ -ray spectra for the  $^{71,73,75}\text{Cu}$  isotopes. The deduced level schemes indicate a reduction of the  $5/2^-$  level energies with increasing neutron number. Such behavior is in agreement with the results of shell model calculations which take into account the increasing  $d_{5/2}-g_{9/2}$  attractive residual interaction due to the filling the  $g_{9/2}$  state. New results have also been obtained for the  $N = 50$  even-even  $^{82}\text{Ge}$  and for the odd  $^{83}\text{As}$  and  $^{81}\text{Ga}$  nuclei. Fig. 3 shows the mass gated  $\gamma$ -ray spectra for these isotopes.

The experimentally determined level energies for  $^{83}\text{As}$ ,  $^{82}\text{Ge}$  and  $^{81}\text{Ga}$  have been compared, for various values of the  $N = 50$  gap energy, with the predictions of shell model calculation obtained allowing  $0p0h$  and  $2p2h$  excitations. Within the shell-model, the description of the nuclear mean field is conventionally obtained by considering the so-called monopole Hamiltonian constructed from the centroids of the two-body interaction. The eigenvalues of this Hamiltonian, usually referred as effective single particle energies, provide the average energies of the specific spherical configurations. They should reproduce the energies of single-proton or single neutron states in odd- $A$  nuclei with  $Z$  or  $N$  equal to a magic number plus or minus one proton or one neutron. The nucleon-nucleon residual interaction, and in particular its tensor force part, changes the spherical single particle energies through the nuclear chart. As already discussed the monopole effect of the tensor force shifts systematically the single-particle levels as protons and neutrons fill certain orbits, the proton-neutron part of the force being the dominant. For the  $Z = 29$  isotopes and  $N = 50$  isotones, due to the strong attraction between particles filling the  $f_{5/2}$  and the  $g_{9/2}$  orbits and the repulsion between the particles filling the  $p_{3/2}$  and the  $g_{9/2}$  orbits one predicts an inversion of the relative position of the  $f_{5/2}-p_{3/2}$  effective single particle states with respect to the usual order, where the  $p_{3/2}$  state is the lowest in excitation energy and the spectra are dominated by the low energy  $\gamma$ -ray corresponding to the  $f_{5/2}-p_{3/2}$  single particle transition. The same mechanism predicts a stabilization or a reinforcement of the  $N = 50$  shell gap. It is interesting to mention here the good agreement obtained between the excitation energies of the newly identified states in  $^{83}\text{As}$ ,  $^{82}\text{Ge}$  and  $^{81}\text{Ga}$  and the results of the shell model calculations, performed using the effective interaction reported in Ref. [23] and an energy gap for the  $N = 50$  shell of 4.7 MeV. [26].

### 1.6. The AGATA Demonstrator experimental campaign

Recently the experimental campaign using the so-called “AGATA Demonstrator” setup has started at LNL [24]. The AGATA Demonstrator is a position sensitive  $\gamma$  detector array composed of up to 5 triple cluster AGATA

detectors mounted in a configuration coupled to the PRISMA spectrometer. Each Ge crystal, individually encapsulated, is 36-fold electrically segmented. Through the use of the segment and pulse shape information, the device can localize the  $\gamma$ -ray interaction point with a spatial resolution of about 5 mm. In the first half year of operation, several experiments have been performed using the AGATA Demonstrator in coincidence either with the PRISMA spectrometer or with other ancillary detectors. In the first experiment, highly collective rotational structures in the  $^{42}\text{Ca}$  nucleus have been populated via Coulomb excitation [25] and their decay has been studied. The aim of the experiment is to determine the  $B(E2)$  strengths for low lying transitions in  $^{42}\text{Ca}$  and, in particular for the super-deformed (SD) band. The knowledge of the electromagnetic transition matrix elements for the inband and outband transitions should allow to extract additional information on the coupling of the SD and yrast bands. The gamma rays with energies up to 2.5 MeV, emitted from the scattered excited nuclei, were detected by the AGATA Demonstrator comprising three triple Ge clusters, in coincidence with the DANTE detectors. The DANTE MCP detectors readout was synchronized and merged with the AGATA data acquisition system using the AGAVA interface. DANTE provided the position of the scattered ions allowing to reconstruct the projectile velocity vector. A preliminary  $\gamma$ -ray spectrum after Doppler correction, reported from Ref. [25], is shown in Fig. 4. The analysis is in progress using more sophisticated tracking algorithms to optimize the response function of the device.

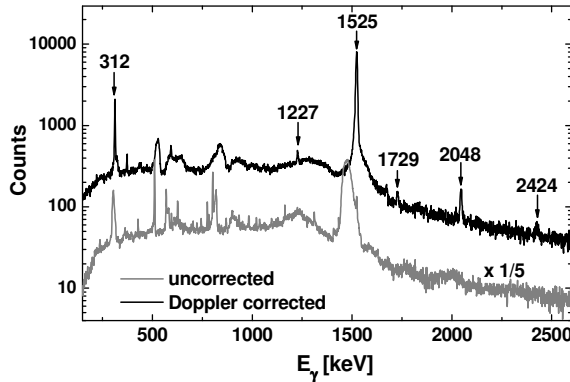


Fig. 4. Preliminary  $\gamma$  spectra (uncorrected and Doppler corrected using DANTE position information) from AGATA Demonstrator. Transitions in  $^{42}\text{Ca}$  are labeled [25].

Several other experiments using the AGATA demonstrator have been focused on lifetime measurements using the RDDS technique. One example concerns the measurements of the  $B(E2)$  strength in the neutron-rich Zn,

Cu and Ni isotopes populated by the  $^{76}\text{Ge}$  induced reaction. In Fig. 5, the  $2^+ \rightarrow 0^+$  562 keV transition in  $^{76}\text{Ge}$  for different target-degrader distances is reported. The two components corresponding to the two different recoil velocities are clearly visible.

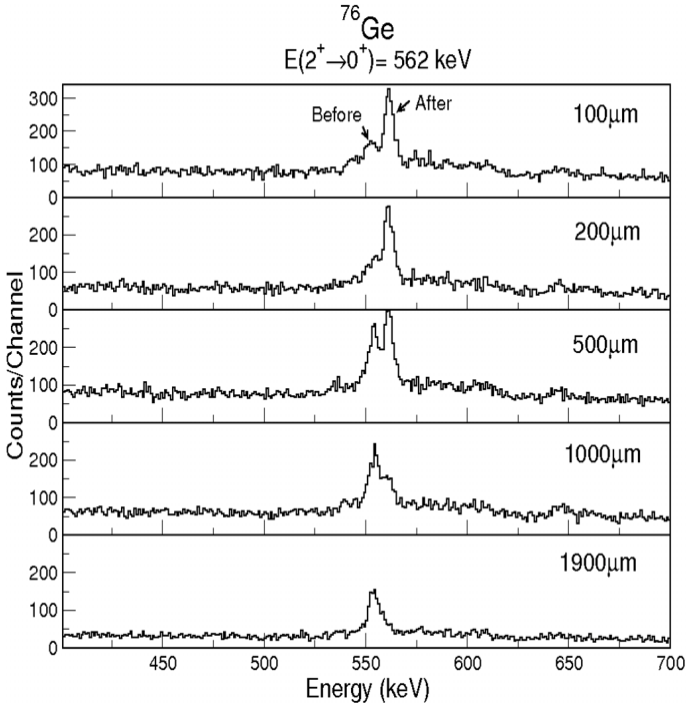


Fig. 5. Doppler-corrected  $\gamma$ -ray spectra showing the  $2^+ \rightarrow 0^+$  562 keV transitions in  $^{76}\text{Ge}$  for different target-degrader distances [27]. The higher and lower energy peaks correspond to the decay after and before the degrader foil.

I would like to thank J. Valiente, E. Farnea, D. Mengoni, E. Sahin, A. Maj, R. Chapman, S. Lunardi and A. Gadea for providing most of the material here reported and to G. Duchene for discussing the results. Many thanks are due to all the colleagues of the LNL accelerator crew and of the PRISMA-CLARA and AGATA groups. This research has been supported by the European Commission through contract number HPRI-CT-1999-00078.

## REFERENCES

- [1] R. Broda, *J. Phys. G: Nucl. Part. Phys.* **32**, R151 (2006).
- [2] A. Gadea *et al.*, *Acta Phys. Pol. B* **38**, 1311 (2007).
- [3] T. Otsuka *et al.*, *Phys. Rev. Lett.* **87**, 082502 (2001).
- [4] T. Otsuka *et al.*, *Phys. Rev. Lett.* **95**, 232502 (2005) and references therein.
- [5] J.I. Prisciandaro *et al.*, *Phys. Lett.* **B510**, 17 (2001).
- [6] A. Gadea *et al.*, *Eur. Phys. J.* **A20**, 193 (2004).
- [7] A.M. Stefanini *et al.*, *Nucl. Phys.* **A701**, 217c (2002).
- [8] A. Poves, J. Retamosa, *Phys. Lett.* **B184**, 311 (1987).
- [9] Z.M. Wang *et al.*, *Phys. Rev.* **C81**, 054305 (2010).
- [10] Z.M. Wang *et al.*, *Phys. Rev.* **C81**, 064301 (2010).
- [11] D. O'Donnell *et al.*, *Phys. Rev.* **C81**, 024318 (2010).
- [12] D.R. Napoli *et al.*, Legnaro Annual Report 2006, INFN-LNL-217(2007), p. 13, and to be published.
- [13] A.M. Nathan *et al.*, *Phys. Rev.* **C16**, 192 (1977).
- [14] R.V.F. Janssens *et al.*, *Phys. Lett.* **B546**, 55 (2002).
- [15] S.N. Liddick *et al.*, *Phys. Rev. Lett.* **92**, 072502 (2004).
- [16] M. Honma *et al.*, *Eur. Phys. J.* **A25**, 499 (2005).
- [17] B. Fornal *et al.*, *Phys. Rev.* **C77**, 014304 (2008).
- [18] J.J. Valiente *et al.*, *Phys. Rev.* **C78**, 024302 (2008).
- [19] J.J. Valiente *et al.*, *Phys. Rev. Lett.* **102**, 242502 (2009).
- [20] D. Mengoni *et al.*, *Phys. Rev.* **C82**, 024308 (2010).
- [21] R. du Rietz *et al.*, *Phys. Rev. Lett.* **93**, 222501 (2004).
- [22] E. Sahin *et al.*, Legnaro Annual Report 2007, INFN-LNL-222(2008), p. 21, and to be published.
- [23] A.F. Lisetskiy, B.A. Brown, M. Horoi, H. Grawe, *Phys. Rev.* **C70**, 044314 (2004).
- [24] A. Gadea *et al.*, *Nucl. Instrum. Methods*, to be published.
- [25] A. Maj *et al.*, LNL Annual Report (2010).
- [26] J.J. Valiente-Dobon *et al.*, *Acta Phys. Pol. B* **37**, 225 (2006).
- [27] E. Sahin *et al.*, private communication.